OPTICA

Quantum-enhanced laser phase noise filter

Ruixin Li,[1] Nanjing Jiao,[1] Bingnan An,[1] Yajun Wang,[1,2,3] Shaoping Shi,[1,2] Long Tian,[1,2] Wei Li,[1,2] and Yaohui Zheng[1,2,4]

[1]State Key Laboratory of Quantum Optics Technologies and Devices, Institute of Opto-Electronics, Shanxi University, Taiyuan 030006, China
[2]Collaborative Innovation Center of Extreme Optics, Shanxi University, Taiyuan, Shanxi 030006, China
[3]YJWangsxu@sxu.edu.cn
[4]yhzheng@sxu.edu.cn

Received 15 July 2025; revised 6 January 2026; accepted 26 January 2026; published 10 February 2026

The direct realization of a quantum-enhanced phase noise filter has remained a major challenge. Conventional techniques are not only plagued by substantial technical noise but also fundamentally constrained by inherent quantum penalty, precluding their direct application in quantum-enhanced noise filtering. This work has realized a practical approach to the first, to our knowledge, quantum-enhanced laser phase noise filter by confronting the key challenges that degrade phase noise extraction and quantum enhancement, specifically the technical noises in the laser's amplitude and phase. Our strategy employs a detuned cavity to direct optical readout of phase noise combined with a hybrid stabilization scheme to suppress both amplitude and phase noises simultaneously. This allows us to circumvent the limitations imposed by quantum noise penalty and effectively enable quantum enhancement via squeezed vacuum injection. Experimentally, we have achieved up to 5 dB of quantum-enhanced phase noise suppression across Fourier frequencies ranging from 5 to 60 kHz. This scheme represents more than just a proof-of-principle—it unlocks the potential of squeezed-enhanced laser phase noise suppression for a broad spectrum of applications.

https://doi.org/10.1364/OPTICA.573701

1. INTRODUCTION

Laser noise is a ubiquitous phenomenon [1] that limits the resolution of optical measurements [2–4] and sensing apparatuses [5–9], as well as the minimum detectable signal [10–14]. Suppressing this noise is therefore a fundamental requirement for achieving unprecedented sensitivity in applications such as gravitational-wave observatories, which must measure displacements on the order of a trillionth of a wavelength [15–17]. Furthermore, in cold-atom trapping, low-noise lasers are critical for minimizing atom heating rates and thereby maximizing experimental coherence times [18,19]. Laser noise, comprising both amplitude and phase noise, originates from fundamental quantum noise due to spontaneous emission and optical losses [20,21], as well as technical noise—classical amplitude and phase fluctuations, which can, in principle, be suppressed to quantum-noise-limited level [22–24]. The continuous pursuit of ultimate sensitivity drives relentless innovation and breakthroughs in laser noise suppression techniques [25,26].

Feedback control is a widely used technique for suppressing laser noise, especially in the low-frequency regime [27–31]. In a typical amplitude noise suppression scheme, part of the laser field is sampled by a photodetector (PD), and the resulting electrical signal is compared with a stable reference to generate an error signal. The noise floor in this configuration includes shot noise from the in-loop sensing beam, electronic noise from the PD, and other technical noise sources coming from the actuator and servo control loop. The extracted amplitude noise serves as the "signal" for the feedback. The achievable signal-to-noise ratio (SNR), defined as the ratio between this "signal" and the noise floor, ultimately limits the noise performance of the out-of-loop field [30,31]. Although considerable efforts have been devoted to improving the SNR—such as developing advanced low-noise, high-saturation-power PDs [23,24], and refined power detection techniques like optical AC coupling [32,33]—the out-of-loop noise performance of such feedback systems cannot exceed the shot noise limit (SNL) of the in-loop sensing beam. To overcome this fundamental barrier, the use of squeezed vacuum states of light was proposed as early as 1987 [34]. This approach leverages the reduced quantum noise in one quadrature of the squeezed vacuum field, thereby improving the measured SNR of amplitude fluctuations without increasing the optical power. After more than three decades, this concept was successfully experimentally demonstrated, achieving laser amplitude stabilization beyond the SNL [35,36].

The direct readout of laser phase noise is not feasible [37–40], presenting a considerable challenge for squeezing-enhanced phase noise suppression. Commonly, phase quadrature information is extracted via two methodologies. The heterodyne detection techniques [39,40], such as Pound–Drever–Hall (PDH) method, is accompanied by a multitude of technical noises—optical (e.g., higher order spatial modes), electronic (e.g., feedback-loop electronics), and mechanical (e.g., vibrations of the frequency discriminator) [30,31]—and are fundamentally constrained by quantum noise penalty, restricting their utility for

quantum-enhanced noise suppression [41–43]. These noise floors complicate the PDH system from achieving quantum enhancement (see Section 3 in Supplement 1 for details). Alternatively, the direct optical readout technique [37,44–46] enables to convert the phase quadrature to an amplitude one, permitting direct detection with a PD. It has an advantage of no quantum noise penalty, but is often impaired by significant technical noise of the optical field, especially under low-efficiency phase readout conditions [47]. The amplitude fluctuations should be effectively mitigated below the SNL with the methodology in Ref. [36] before quantum-enhanced phase noise stabilization. Meanwhile, to gain the maximum quantum advantage, the readout unit should be carefully designed to balance the internal loss, phase-to-amplitude conversion efficiency, and readout frequency bandwidth. To realize the quantum-enhanced regime, we must have a deep understanding of the physical mechanism in noise readout and suppression processes, and provide the essential conditions to exceed the fundamental limit—SNL.

In this work, we have established a complete theoretical model and reported the first experimental demonstration of a squeezing-enhanced laser phase noise filter. Based on a noise ellipse rotation scheme [37,44–46], we have partially extracted the phase noise reflected by a one-ended cavity. Before phase noise filtering, the amplitude noise was pre-stabilized close to the SNL across the kHz to MHz frequency range, thereby substantially reducing its impact on phase noise extraction. Finally, a squeezing-enhanced phase noise stabilization was realized, exhibiting a maximum noise reduction improvement of 5 dB in the Fourier frequency range from 5 to 60 kHz. It paves the way for further phase noise reduction via quantum-enhanced techniques.

2. QUANTUM-ENHANCED ACTIVE FEEDBACK THEORY

The underlying physical mechanism of our quantum-enhanced phase noise filter is illustrated in Fig. 1. First, we compare it with the amplitude noise stabilization methodology, where noise can be directly detected using a low-noise PD, as shown in Fig. 1(a). Under high-gain feedback, the amplitude noise is finally limited by the vacuum noise, coupled from the input port of the beam splitter (BS1), which becomes the fundamental limit for further noise improving [34,35]. If the vacuum field is replaced by an audio-band squeezed vacuum, this fundamental limit can be overcome—being stabilized beyond the SNL [35]. Subsequently, in phase noise stabilization, more complex technical noises—optical, electronic, mechanical, and quantum noise penalty [28–31,41] introducted during phase extracting, contribute the noise floor of the in-loop unit. How to remove or circumvent these technical noises is the key issue. Inspired by the direct readout concept illustrated in Fig. 1(a), we have developed a direct phase noise readout unit, utilizing a noise ellipse rotation technique to construct the quantum-enhanced phase noise filter, as depicted in Fig. 1(b). This technique partially converts the phase quadrature into an amplitude one, vice versa. Then, the phase noise can be directly extracted by a PD without the disturbing of electronic and mechanical noises and quantum noise penalty. But, due to the small rotation angle of the noise ellipse in the low-frequency range, a residual amplitude noise sneaks into the PD, and degrades the SNR in phase noise extraction. Therefore, it is essential to suppress this residual noise as much as possible prior to squeezing injection.

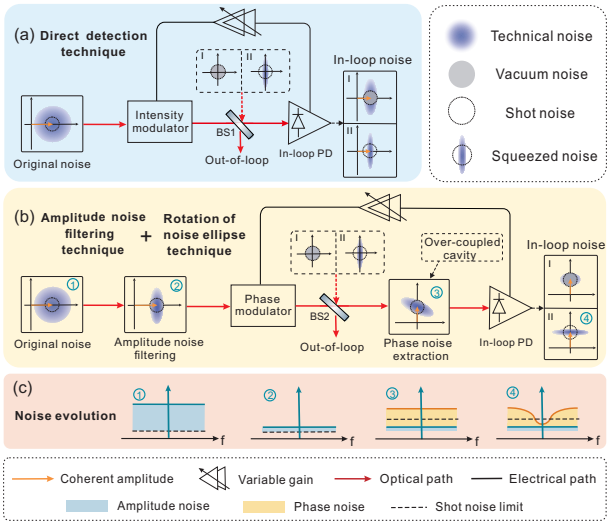

Fig. 1. Physical mechanism of the quantum-enhanced laser noise filter with an active feedback control loop. (a) Amplitude noise suppression via active feedback control with direct detection of the laser power; (b) quantum-enhanced phase noise suppression using a noise ellipse rotation technique combined with amplitude noise pre-stabilization; and (c) noise evolution of the amplitude quadrature in the sideband picture (expressed in relative noise units), corresponding to the configuration shown in (b). BS, beam splitter; PD, photodetector.

To address this, we implement an amplitude noise filter operating at the SNL noise level to improve the SNR, as shown in Figs. 1(b) and 1(c).

We begin our analysis of the quantum-enhanced phase-noise filter under pre-stabilized amplitude noise condition (position ②). The laser field first passes through a phase modulator, after which it is coupled with a squeezed vacuum on a BS2 with power transmission t and reflection r. The combined field serves as the in-loop sensing beam, and its amplitude and phase quadratures are given by

$$\begin{aligned} X_{\text{in-loop}} &= \sqrt{t}X_{\text{in}} + \sqrt{r}X_S\cos\theta_p + \sqrt{r}Y_S\sin\theta_p \\ Y_{\text{in-loop}} &= \sqrt{t}Y_{\text{in}} + \sqrt{r}Y_S\cos\theta_p - \sqrt{r}X_S\sin\theta_p \end{aligned}, \tag{1}$$

where X_{in} and Y_{in} are the amplitude and phase quadratures of the input field on the BS2, respectively, and X_S and Y_S are that of the squeezed vacuum. θ_p is the relative phase between the squeezed vacuum and the input beam. Then, the combined field is injected into an over-coupled cavity (OCC, position ③) to implement a frequency-dependent quadrature-rotation. The output field of the OCC serves as the feedback error signal, whose amplitude quadrature becomes

$$X^d_{\text{in-loop}} = X_{\text{in-loop}}\cos\theta_1 + Y_{\text{in-loop}}\sin\theta_1, \tag{2}$$

where θ_1 is the noise ellipse rotation angle determined by the cavity detuning. Here, the coherent field is rotated by 90° in the OCC, but its phase quadrature is changed with an angle θ_1 relative to the coherent field (position ③, see Section 1 in Supplement 1 for details). As a result, part of the phase quadrature is converted into an amplitude one, which can be directly measured by a PD. Meanwhile, the residual amplitude noise transferred from the input field also contributes the noise floor of the PD and becomes a new technical noise source in the feedback control loop.

Substituting Eq. (1) into Eq. (2) yields

$$X^d_{\text{in-loop}} = \sqrt{t}X_{\text{in}}\cos\theta_1 + \sqrt{t}Y_{\text{in}}\sin\theta_1 + \sqrt{r}X_S\cos(\theta_p+\theta_1) + \sqrt{r}Y_S\sin(\theta_p+\theta_1). \quad (3)$$

If we chose $\theta_p = -\theta_1$, the contribution of the anti-squeezing quadrature [the term proportional to Y_S in Eq. (3)] is eliminated. Hence, we can obtain the quantum-enhanced phase noise suppression without disturbing the antisqueezing quadrature.

The amplitude quadrature of the laser field at the OCC output contains both the converted phase and residual amplitude components. The measured noise by the PD is thus expressed as relative intensity noise (RIN): $2h\nu S^{X,Y}/P_{\text{in}} = \text{RIN}^2_{X,Y}$, where h is the Planck's constant, ν is the optical carrier frequency, and P_{in} is the incident optical power, and the noise variances are defined as $S^{X,Y} = X^2, Y^2$. Under the condition of $\omega \ll \kappa_1$, the rotation angle is approximately equal to $\theta_1 \approx \omega/\kappa_1$, where ω is the analysis frequency, and κ_1 is the linewidth of the OCC (see Section 1 in Supplement 1 for details). Then, Eq. (3) expressed in the RIN unit becomes [48]

$$\text{RIN}^2_{\text{in-loop}} = \frac{2h\nu}{P_{\text{in-loop}}}\left(tS^X_{\text{in}} + t\frac{\omega^2}{\kappa_1^2}S^Y_{\text{in}} + rS^X_S\right), \quad (4)$$

where $P_{\text{in-loop}}$ is the in-loop optical power, and the quantity $2h\nu/P_{\text{in-loop}} = \text{RSN}^2_{\text{in-loop}}$ represents the relative shot noise (RSN) of the in-loop optical field. Here, S^X_{in} corresponds to the amplitude noise variance of the input optical field, and S^X_S is that of the squeezed vacuum field.

Equation (4) can be simplified using RIN and RSN notations as

$$\text{RIN}^2_{\text{in-loop}} = \text{RIN}^2_X + \frac{\omega^2}{\kappa_1^2}\text{RIN}^2_Y + \text{RSN}^2_{\text{in-loop}}\cdot rS^X_S. \quad (5)$$

In this expression, RIN^2_X corresponds to the residual amplitude noise after power pre-stabilization at position ②. The second term describes the converted phase noise at position ③, while the third term is governed by the shot noise of the in-loop optical field and the injected squeezed vacuum (position ④). Clearly, the first two terms contribute to the technical noise within the feedback control loop. To ensure the activation of quantum enhancement, these noises must be suppressed well below the noise floor of the third term. Using the same noise readout method, the measured RIN of the out-of-loop phase noise can be expressed as (see Section 2 in Supplement 1 for details)

$$\text{RIN}^2_{\text{out-of-loop}} \approx \text{RIN}^2_X + \frac{\omega^2}{\kappa_2^2}\text{RIN}^2_Y, \quad (6)$$

where κ_2 denotes the linewidth of the impedance-matched cavity (IMC) in the out-of-loop.

Under the action of feedback control, the out-of-loop RIN normalized to the in-loop reference evolves as (see Section 2 in Supplement 1 for details)

$$\text{RIN}^2_{\text{out-of-loop}} \approx \text{RIN}^2_X + \frac{\theta_1^2\text{RIN}^2_Y}{\left|1-\theta_1\sqrt{t}G(\omega)\right|^2} + \text{RSN}^2_{\text{in-loop}}\cdot rS^X_S + \text{RSN}^2_{\text{in-loop}}S^e_{\text{il-PD}}, \quad (7)$$

where $G(\omega)$ is the frequency-dependent feedback gain. The first term in Eq. (7) corresponds to the amplitude noise of the optical field, which sets the SNR limit for phase noise suppression. The second term reflects the residual phase noise after feedback. The third term is determined by the shot noise of the in-loop optical field and the injected squeezed vacuum. The fourth term is the electronic noise of the in-loop PD.

3. EXPERIMENTAL SETUP

The experimental setup for quantum-enhanced phase noise filter is illustrated in Fig. 2. A single-frequency fiber laser operating at 1550 nm with an output power of 1 W serves as the light source for subsequent experiments. The laser output passes through an acousto-optic modulator (AOM) with a frequency shift of 110 MHz and a diffraction efficiency of 50%, enabling fast phase modulation within a 200 kHz bandwidth. The majority of the optical power (approximately 500 mW) then travels through an optical isolator (ISO) and enters a second harmonic generator (SHG), where it is converted to 775 nm. This frequency-doubled output serves as the pump field for parametric down-conversion in a doubly resonant optical parametric oscillator (OPO). Detailed descriptions of the SHG and OPO systems, including their design, operation, and control schemes, can be found in Refs. [49–51]. By adjusting the pump power using a half-wave plate (HWP2) and a polarizing beam splitter (PBS2), the pump power injected into the OPO is set to 11.5 mW—well below the OPO's oscillation threshold of 20 mW. The generated squeezed vacuum is −10.6 dB, which is directly measured by an independent audio-band balanced homodyne detector (BHD) closing to the dichroic beam splitter (DBS2) [50]. Its is separated from the pump light using the DBS2.

Notably, the SHG also functions as an amplitude noise suppressor. Its operating mechanism relies on the nonlinear relationship induced by the frequency conversion process between the intracavity circulating power and the reflected power of the fundamental wave [49,52]. Maximum amplitude noise reduction is achieved when the slope of this nonlinear transfer function approaches zero, enabling amplitude noise suppression close to the SNL across the kHz–MHz frequency range at a conversion efficiency of 70% [49,52]. This effectively eliminates the influence of amplitude noise on downstream phase noise suppression (position ① → ②). The reflected fundamental wave from the SHG, with a power of 100 mW, is first attenuated to 5 mW using a HWP1 and a PBS1. It is then directed into a BS with a power reflectivity of $r = 99\%$, which divides the beam into in-loop and out-of-loop

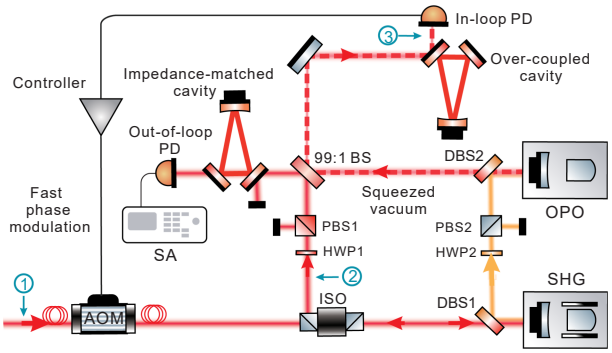

Fig. 2. Schematic of the experimental setup for the quantum-enhanced phase noise filter. AOM, acousto-optic modulator; ISO, optical isolator; SHG, second-harmonic generator; DBS, dichroic beam splitter; OPO, optical parametric oscillator; HWP, half-wave plate; PBS, polarizing beam splitter; PD, photodetector; 99:1 BS, 99:1 beam splitter; SA, spectrum analyzer.

paths. Approximately 50 μW of the in-loop beam is injected into an OCC, serving as a phase-to-amplitude quadrature converter (position ③). An amplitude-squeezed vacuum is coupled with the in-loop laser beam at the 99:1 BS, and a mode-matching efficiency between them is about 98.5 ± 0.2%. The OCC consists of an input coupler with 93.8% power reflectivity, an output coupler with 99.7% reflectivity, and a concave mirror with a high reflectivity >99.95%. Its cavity length is 426 mm, and results in a cavity linewidth of 7.5 MHz. This design ensures sufficient transmitted power for robust cavity-detuning locking using the fringe-side locking technique [53].

Phase noise is extracted by the PD at the reflected port of the OCC. The resulting photocurrent is fed back to the upstream AOM via a PID controller (Vescent, D2-125) to actively suppress the phase noise. However, the transmittance of the OCC introduces additional loss for the squeezed vacuum field, which degrades the quantum-enhanced noise suppression level. To balance the phase-to-amplitude noise conversion efficiency with the transmission loss, the OCC is locked at approximately 1.5 times linewidth point, introducing only 1.6% additional loss (see Section 4 in Supplement 1 for experiment details). Under this condition, the quadrature rotation angle becomes $\theta_1 \cong 0.1 \cdot \omega/\kappa_1$. To achieve optimal quantum-enhanced noise suppression, the relative phase between the squeezed vacuum and the input field at the BS is precisely locked to $-\theta_1 \approx 0$ with a coherent control technique [54]. The out-of-loop phase noise is characterized using an independent, half-detuned, three-mirror IMC. Its operating principle is identical to that of the OCC, but it features a linewidth of 6.8 MHz due to the 97% power reflectivity of its two plane mirrors.

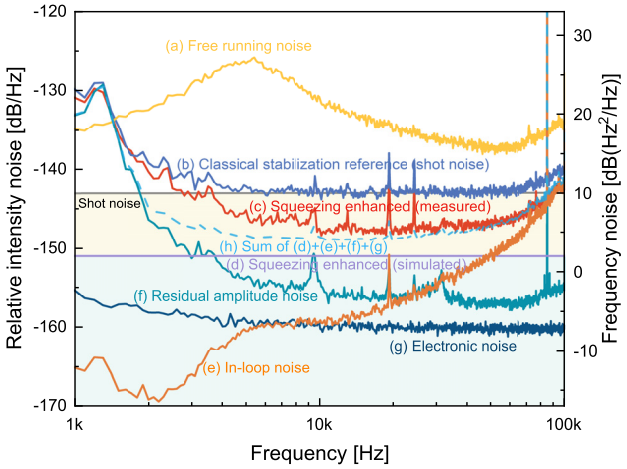

Fig. 3. Experimental results and noise budget of the quantum-enhanced laser phase filter. Trace (a): measured free-running laser frequency noise. Trace (b): measured out-of-loop laser frequency noise corresponding to the shot noise level of the 50 μW in-loop detected power, representing the classical stabilization reference. Trace (c): nonclassical laser frequency noise reduction, showing an average of 5 dB below the shot-noise level between 5 and 60 kHz. Trace (d): simulated squeezing enhancement. Trace (e): in-loop noise during squeezing-enhanced electronic loop operation. Trace (f): residual amplitude noise. This result is from a direct measurement performed prior to phase-to-amplitude conversion with a detection power of 5 mW. Trace (g): electronic noise of the in-loop PD. Trace (h): uncorrelated sum of the noise sources from (d), (e), (f), and (g). All measurements were performed using a spectrum analyzer (R&S FSW) across Fourier frequencies from 1 to 100 kHz, with a resolution bandwidth (RBW) of 100 Hz and video bandwidth (VBW) of 10 Hz.

4. EXPERIMENTAL RESULTS AND DISCUSSION

In the experimental results, we describe the phase noises in the RIN and frequency noise units simultaneously. The former one is the natural consequence of the theoretical derivation from Eqs. (1)–(7), and the latter one is used to present the real frequency noise level of our system. The conversion between the two units can be found in Section 5 of Supplement 1 for details. First, a free-running laser with 5 mW is passively power stabilized to −157 dB/Hz by the SHG, compared with a shot noise level of −162.9 dB/Hz [49]. It is directly measured by a PD before it injected into the feedback control loop, as shown in trace (f). However, limited by the noise suppression ability of the phase noise control loop, only a 50 μW pre-stabilized laser field is extracted as the in-loop sensing beam. Its shot noise is limited to −142.9 dB/Hz. Apparently, the amplitude noise of the laser field is 14.1 dB lower than the shot noise level of the in-loop field. This corresponds to the amplitude-noise term in Eq. (7), which determines the lower bound noise floor in phase noise readout, and sets the final SNR for quantum-enhanced stabilization. Second, its phase noise is directly measured by using the IMC, shown as trace (a) of Fig. 3. When the feedback control loop is activated, the in-loop noise is actively suppressed, as illustrated in trace (e), corresponding to the second term in Eq. (7). Once this in-loop noise is reduced below its SNL, the dominant contribution to the out-of-loop spectrum shifts from the technical noise to the quantum one associated with the detected shot noise—the third term in Eq. (7) with $S_S^X = 1$. The out-of-loop noise is constrained to −142.9 dB/Hz, as observed in trace (b). By injecting an amplitude-squeezed vacuum ($S_S^X < 1$) at the 99:1 BS, the SNL is surpassed and further phase noise suppression is enabled. As shown in trace (c), the phase noise reduction is improved by 5 dB between 5 and 60 kHz. Trace (g) shows the electronic noise of the in-loop PD, which is approximately −160 dB/Hz (last term of Eq. (7)).

Based on Eq. (7), the quantum enhancement is related to a noise coupling term and a squeezed vacuum term. The noise coupling is induced by the residual amplitude and phase noises and the electronic noise of the in-loop PD. The squeezed vacuum could be deteriorated by optical losses and phase fluctuations in the squeezed vacuum generation, propagation, and detection. Therefore, we can conclude that the discrepancy between the generated squeezed vacuum and the observed quantum enhancement arises from the optical losses, phase fluctuations, and noise coupling, as summarized in Table 1. Individual contributions of the system losses are also listed, corresponding to a 1.9 dB degradation of the squeezing strength [35]. The three phase-locking loops introduce a total phase fluctuation of 20 ± 0.9 mrad, which are directly and individually measured by the rms noise of the error signal of their locking circuits [55]. It results in an additional 0.6 dB reduction in squeezing performance, due to the anti-squeezing noise coupling from the phase fluctuation [56]. Considering only optical losses and phase fluctuations in the squeezed state generation, the theoretically achievable quantum enhancement is 8.1 dB, predicted by Eq. (7) and shown in trace (d). Furthermore, the feedback process introduces additional noise coupling from the PD's electronic noise [trace (g)], residual amplitude noise [trace (f)], and the residual phase noise of the in-loop [trace (e)]. After comprehensive consideration, these noise sources contribute to a further 2.2 dB degration in quantum enhancement, lowering the theoretically achievable value to 5.9 dB, as indicated by trace (h). Finally,

Table 1. Noises and System Errors Budget from the Optical Loss, Phase Fluctuation, and Noise Coupling

Optical Loss	Value (%)	System Loss (dB)
OPO escape efficiency	97 ± 0.5	1.9
Efficiency of interference	98.5 ± 0.2	
Quantum efficiency of PD	99 ± 0.2	
Over-coupled cavity	98.4 ± 0.5	
Laser propagation efficiency	96 ± 0.5	
Total efficiency	88 ± 0.8	
Phase Fluctuation	**Value (mrad)**	**System Loss (dB)**
OPO cavity length	2 ± 0.3	0.6
Relative phase of squeezed and frequency-shifted light	7 ± 0.5	
Relative phase of squeezed and local oscillator light	11 ± 0.6	
Total phase fluctuation	20 ± 0.9	
Noise-Coupling	**Value (%)**	**System Loss (dB)**
Electronic noise	2.3 ± 0.1	2.2
Laser amplitude noise	6.2 ± 0.2	
In-loop phase noise	2.1 ± 0.5	
Total cross-coupling	10.6 ± 0.8	

we observed a zero drift phenomenon in the OPO, SHG, OCC, and IMC cavity lengths as well as the relative phases locking error signals under noise feedback control operation, which introduces fluctuations in the phase or amplitude quadrature of the output laser field. These fluctuations couple the anti-squeezed or directly transmit into the squeezed quadrature in the phase noise readout process, and further degrade the measured outcome, resulting in a final quantum enhancement of 5 dB. The elevated noise coupling below 10 kHz is primarily attributed to cavity detuning of the SHG within its locking bandwidth, induced by modulation from the upstream AOM during phase noise feedback. We anticipate that advancements in photodetector, actuation elements, and servo loop design will furtherly broaden the feedback bandwidth and increase the phase noise reduction level [36].

5. CONCLUSION AND OUTLOOK

We have reported the first experimental demonstration of a quantum-enhanced laser phase noise filter. Using a hybrid noise stabilization scheme, the technical noise level in the output laser field of the OCC was suppressed to a sub-SNL of the in-loop laser beam. Combing with the optical direct readout technique of phase noise, the essential conditions for squeezing enhancement was created. With the injection of a 10.6 dB squeezed vacuum, we have achieved up to 5 dB of quantum-enhanced phase noise suppression within the Fourier frequency range of 5 to 60 kHz. The experimental results were also predicted by the theoretical model. This work opens the way for applying squeezed vacuum states to laser phase noise reduction and offers a promising approach for advancing quantum metrology and precision measurement.

Funding. National Natural Science Foundation of China (62225504, U22A6003, 62027821, 62375162); National Key Research and Development Program of China (2024YFF0726401).

Disclosures. The authors declare no conflicts of interest.

Data availability. Data underlying the results presented in this paper are not publicly available at this time but may be obtained from the authors upon reasonable request.

Supplemental document. See Supplement 1 for supporting content.

REFERENCES

1. J. L. Hall, "Nobel Lecture: Defining and measuring optical frequencies," Rev. Mod. Phys. **78**, 1279–1295 (2006).
2. A. Hugi, G. Villares, S. Blaser, *et al.*, "Mid-infrared frequency comb based on a quantum cascade laser," Nature **492**, 229–233 (2012).
3. Y. Y. Jiang, A. D. Ludlow, N. D. Lemke, *et al.*, "Making optical atomic clocks more stable with 10^{-16} level laser stabilization," Nat. Photonics **5**, 158–161 (2011).
4. M. Jing, Y. Hu, J. Ma, *et al.*, "Atomic superheterodyne receiver based on microwave-dressed Rydberg spectroscopy," Nat. Phys. **16**, 911–915 (2020).
5. C. L. Degen, F. Reinhard, and P. Cappellaro, "Quantum sensing," Rev. Mod. Phys. **89**, 035002 (2017).
6. S. Shi, L. Tian, Y. Wang, *et al.*, "Demonstration of channel multiplexing quantum communication exploiting entangled sideband modes," Phys. Rev. Lett. **125**, 070502 (2020).
7. X. Sun, Y. Wang, Y. Tian, *et al.*, "Deterministic and universal quantum squeezing gate with a teleportation-like protocol," Laser Photonics Rev. **16**, 2100329 (2022).
8. S. Shi, Y. Wang, L. Tian, *et al.*, "Continuous variable quantum teleportation network," Laser Photonics Rev. **17**, 2200508 (2023).
9. X. Fang, Y. Zhu, X. Cai, *et al.*, "Overcoming laser phase noise for low-cost coherent optical communication," Nat. Commun. **15**, 6339 (2024).
10. L. Gao, L. Zheng, B. Lu, *et al.*, "Generation of squeezed vacuum state in the millihertz frequency band," Light Sci. Appl. **13**, 294 (2024).
11. J. Heinze, B. Willke, and H. Vahlbruch, "Observation of squeezed states of light in higher-order Hermite-Gaussian modes with a quantum noise reduction of up to 10 dB," Phys. Rev. Lett. **128**, 083606 (2022).
12. H. Yu, L. McCuller, M. Tse, *et al.*, "Quantum correlations between light and the kilogram-mass mirrors of LIGO," Nature **583**, 43–47 (2020).
13. M. Korobko, L. Kleybolte, S. Ast, *et al.*, "Beating the standard sensitivity-bandwidth limit of cavity-enhanced interferometers with internal squeezed-light generation," Phys. Rev. Lett. **118**, 143601 (2017).
14. X. Zuo, Z. Yan, Y. Feng, *et al.*, "Quantum interferometer combining squeezing and parametric amplification," Phys. Rev. Lett. **124**, 173602 (2020).
15. S. L. Danilishin, F. Y. Khalili, and H. Miao, "Advanced quantum techniques for future gravitational-wave detectors," Living Rev. Relativ. **22**, 2 (2019).
16. M. Tse, H. Yu, N. Kijbunchoo, *et al.*, "Quantum-enhanced advanced LIGO detectors in the era of gravitational-wave astronomy," Phys. Rev. Lett. **123**, 231107 (2019).
17. J. Lough, E. Schreiber, F. Bergamin, *et al.*, "First demonstration of 6 dB quantum noise reduction in a kilometer scale gravitational wave observatory," Phys. Rev. Lett. **126**, 041102 (2021).
18. Z. Meng, L. Wang, W. Han, *et al.*, "Atomic Bose-Einstein condensate in twisted-bilayer optical lattices," Nature **615**, 231–236 (2023).
19. M. E. Gehm, K. M. O'Hara, T. A. Savard, *et al.*, "Dynamics of noise-induced heating in atom traps," Phys. Rev. A **58**, 3914–3921 (1998).
20. M. Heurs, V. M. Quetschke, B. Willke, *et al.*, "Simultaneously suppressing frequency and intensity noise in a Nd:YAG nonplanar ring oscillator by means of the current-lock technique," Opt. Lett. **29**, 2148–2150 (2004).
21. Y. Tian, Y. Wang, W. Wang, *et al.*, "Reservoir-engineered squeezed lasing through the parametric coupling," Phys. Rev. Lett. **134**, 243803 (2025).
22. E. H. Huntington, C. C. Harb, M. Heurs, *et al.*, "Quantum noise limits to simultaneous quadrature amplitude and phase stabilization of solid-state lasers," Phys. Rev. A **75**, 013802 (2007).
23. P. Kwee, B. Willke, and K. Danzmann, "Shot-noise-limited laser power stabilization with a high-power photodiode array," Opt. Lett. **34**, 2912–2914 (2009).
24. J. Junker, P. Oppermann, and B. Willke, "Shot-noise-limited laser power stabilization for the AEI 10 m Prototype interferometer," Opt. Lett. **42**, 755–758 (2017).
25. J. Aasi, J. Abadie, B. P. Abbott, *et al.*, "Enhanced sensitivity of the LIGO gravitational wave detector by using squeezed states of light," Nat. Photonics **7**, 613–619 (2013).
26. R. Schnabel, "Squeezed states of light and their applications in laser interferometers," Phys. Rep. **684**, 1–51 (2017).

27. Y. X. Chao, Z. X. Hua, X. H. Liang, *et al.*, "Pound–Drever–Hall feedforward: laser phase noise suppression beyond feedback," Optica **11**, 945–952 (2024).
28. M. H. Idjadi and F. Aflatouni, "Nanophotonic phase noise filter in silicon," Nat. Photonics **14**, 234–239 (2020).
29. M. H. Idjadi, K. Kim, and N. K. Fontaine, "Modulation-free laser stabilization technique using integrated cavity-coupled Mach-Zehnder interferometer," Nat. Commun. **15**, 1922 (2024).
30. F. Meylahn, N. Knust, and B. Willke, "Stabilized laser system at 1550 nm wavelength for future gravitational-wave detectors," Phys. Rev. D **105**, 122004 (2022).
31. R. Li, N. Jiao, B. An, *et al.*, "Optimizing frequency noise calibration and manipulation in an active feedback control loop," Opt. Laser Technol. **174**, 110617 (2024).
32. P. Kwee, B. Willke, and K. Danzmann, "Optical ac coupling to overcome limitations in the detection of optical power fluctuations," Opt. Lett. **33**, 1509–1511 (2008).
33. S. Kaufer and B. Willke, "Optical AC coupling power stabilization at frequencies close to the gravitational wave detection band," Opt. Lett. **44**, 1916–1919 (2019).
34. C. M. Caves, "Squeezing more out of a laser," Opt. Lett. **12**, 971–973 (1987).
35. H. Vahlbruch, D. Wilken, M. Mehmet, *et al.*, "Laser power stabilization beyond the shot noise limit using squeezed light," Phys. Rev. Lett. **121**, 173601 (2018).
36. R. Li, B. An, N. Jiao, *et al.*, "Bright squeezed light in the kilohertz frequency band," Light Sci. Appl. **14**, 310 (2025).
37. A. S. Villar, "The conversion of phase to amplitude fluctuations of a light beam by an optical cavity," Am. J. Phys. **76**, 922–929 (2008).
38. X. Xie, R. Bouchand, D. Nicolodi, *et al.*, "Phase noise characterization of sub-hertz linewidth lasers via digital cross correlation," Opt. Lett. **42**, 1217–1220 (2017).
39. F. Schmid, J. Weitenberg, T. W. Hänsch, *et al.*, "Simple phase noise measurement scheme for cavity-stabilized laser systems," Opt. Lett. **44**, 2709–2712 (2019).
40. E. D. Black, "An introduction to Pound–Drever–Hall laser frequency stabilization," Am. J. Phys. **69**, 79–87 (2001).
41. T. Zhang, D. Martynov, A. Freise, *et al.*, "Quantum squeezing schemes for heterodyne readout," Phys. Rev. D **101**, 124052 (2020).
42. T. Zhang, P. Jones, J. Smetana, *et al.*, "Two-carrier scheme: evading the 3 dB quantum penalty of heterodyne readout in gravitational-wave detectors," Phys. Rev. Lett. **126**, 221301 (2021).
43. D. W. Gould, V. B. Adya, S. S. Y. Chua, *et al.*, "Quantum enhanced balanced heterodyne readout for differential interferometry," Phys. Rev. Lett. **133**, 063602 (2024).
44. M. D. Levenson, R. M. Shelby, and S. H. Perlmutter, "Squeezing of classical noise by nondegenerate four-wave mixing in an optical fiber," Opt. Lett. **10**, 514–516 (1985).
45. P. Galatola, L. A. Lugiato, M. G. Porreca, *et al.*, "System control by variation of the squeezing phase," Opt. Commun. **85**, 95–103 (1991).
46. J. Liu and I. Yamaguchi, "Analysis of fringe locking in a laser diode interferometer under injection-current modulation," Opt. Lett. **24**, 336–338 (1999).
47. W. Nagourney, *Quantum Electronics for Atomic Physics and Telecommunication* (Oxford University, 2014).
48. J. R. Venneberg and B. Willke, "Quantum correlation measurement of laser power noise below shot noise," Opt. Continuum **1**, 1077–1084 (2022).
49. N. Jiao, R. Li, B. An, *et al.*, "Passive laser power stabilization in a broadband noise spectrum via a second-harmonic generator," Opt. Lett. **49**, 3568–3571 (2024).
50. W. Zhang, J. Wang, Y. Zheng, *et al.*, "Optimization of the squeezing factor by temperature-dependent phase shift compensation in a doubly resonant optical parametric oscillator," Appl. Phys. Lett. **115**, 241101 (2019).
51. Y. Wang, W. Zhang, R. Li, *et al.*, "Generation of −10.7 dB unbiased entangled states of light," Appl. Phys. Lett. **118**, 084001 (2021).
52. Y. Li, F. Seddighi, and G. Porat, "Broadband suppression of laser intensity noise based on second-harmonic generation," Phys. Rev. Appl. **22**, 014026 (2024).
53. N. Jiao, R. Li, Y. Wang, *et al.*, "Laser phase noise suppression and quadratures noise intercoupling in a mode cleaner," Opt. Laser Technol. **154**, 108303 (2022).
54. H. Vahlbruch, S. Chelkowski, B. Hage, *et al.*, "Coherent control of vacuum squeezing in the gravitational-wave detection band," Phys. Rev. Lett. **97**, 011101 (2006).
55. T. Aoki, G. Takahashi, and A. Furusawa, "Squeezing at 946 nm with periodically poled $KTiOPO_4$," Opt. Express **14**, 6930–6935 (2006).
56. W. Yang, S. Shi, Y. Wang, *et al.*, "Detection of stably bright squeezed light with the quantum noise reduction of 12.6 dB by mutually compensating the phase fluctuations," Opt. Lett. **42**, 4553–4556 (2017).